Article

Synthesis of Helical Polyacetylene in Chiral Nematic Liquid Crystals Using Crown Ether Type Binaphthyl Derivatives as Chiral Dopants

Kazuo Akagi, Shouxue Guo, Taizou Mori, Munju Goh, Guangzhe Piao, and Mutsumasa Kyotani

J. Am. Chem. Soc., **2005**, 127 (42), 14647-14654• DOI: 10.1021/ja051548e • Publication Date (Web): 01 October 2005

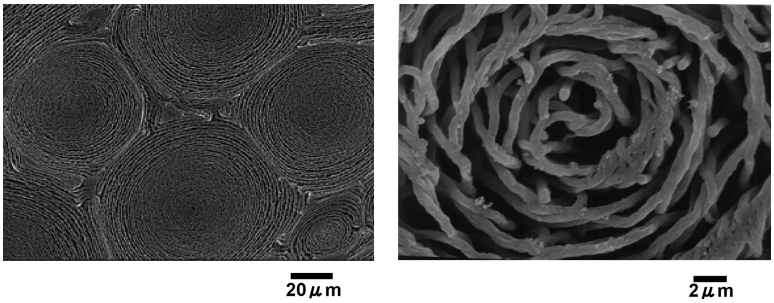

More About This Article

Additional resources and features associated with this article are available within the HTML version:

- Supporting Information
- Links to the 15 articles that cite this article, as of the time of this article download
- Access to high resolution figures
- Links to articles and content related to this article
- Copyright permission to reproduce figures and/or text from this article

View the Full Text HTML

J|A|C|S
ARTICLES
Published on Web 10/01/2005

Synthesis of Helical Polyacetylene in Chiral Nematic Liquid Crystals Using Crown Ether Type Binaphthyl Derivatives as Chiral Dopants

Kazuo Akagi,*[,†,‡] Shouxue Guo,[†] Taizou Mori,[†] Munju Goh,[†] Guangzhe Piao,[†] and Mutsumasa Kyotani[‡]

Contribution from the Institute of Materials Science, and Tsukuba Research Center for Interdisciplinary Materials Science (TIMS), University of Tsukuba, Ibaraki 305-8573, Japan

Received March 10, 2005; E-mail: akagi@ims.tsukuba.ac.jp

Abstract: A series of crown ether type binaphthyl derivatives (CEBDs) were synthesized and used as chiral dopants to induce chiral nematic (N*) liquid crystals (LCs). The twisting powers of the CEBDs for phenylcyclohexane (PCH)-derived nematic LCs were evaluated. It was found that the twisting powers of the CEBDs increased with decreasing ring size of the crown ether. Helical polyacetylenes were synthesized in the N*-LCs induced by the CEBDs. The relationship between the morphology of the helical polyacetylene and the helical structure of the N*-LC was investigated. The result showed that the interdistance between the fibril bundles of the helical polyacetylene was equal to a half-helical pitch of the N*-LC and the screw direction of the polyacetylene fibrils was opposite to that of the N*-LC.

1. Introduction

Polyacetylene is a prototype of an electrical conductive polymer because of its linear conjugated molecular structure.[1] Since discoveries for the synthesis of polyacetylene film[2] and the evolution of electrical conductivity upon chemical doping,[3] polyacetylene, as well as other kinds of conjugated polymers, has been extensively investigated from aspects of novel synthesis and electrical and optical properties.[4] It has been generally accepted that polyacetylene has a planar structure, irrespective of cis and trans forms, due to strong π-conjugation between the sp^2-hybridized carbon atoms in the polymer chain.[1,5] On the other hand, strong interchain interaction gives rise to a fibrillar crystal consisting of rigidly π-stacked polymer chains. This makes polyacetylene infusible and insoluble in any kind of solvent. Thus, the solid-state structure and morphology of polyacetylene are determined during acetylene polymerization, which is quite different from substituted polyacetylene in terms of fusibility and solubility.[6] Besides, the fibril morphology of polyacetylene film is randomly oriented, as is usually encountered in ordinary polymers, depressing the inherent one-dimensionality of this polymer. Hence, several kinds of procedures and polymerization methods for macroscopic alignment of morphology have been developed to achieve higher electrical conductivity with anisotropic nature.[7,8] Introduction of a liquid crystal (LC) group into the side chain of polyacetylene is one approach to align the polymer under an external force such as shear stress, rubbing, or a magnetic field.[9−11] The use of nematic LC as a solvent gave us directly aligned polyacetylene with the aid of gravity flow or a magnetic field.[12,13]

[†] Institute of Materials Science.

[‡] Tsukuba Research Center for Interdisciplinary Materials Science.

(1) Chien, J. C. W. In *Polyacetylene—Chemistry, Physics and Material Science*; Academic Press: London, 1984; Chapter 2.

(2) Ito, T.; Shirakawa, H.; Ikeda, S. *J. Polym. Sci., Polym. Chem. Ed.* **1974**, *12*, 11.

(3) (a) Shirakawa, H.; Louis, E.; MacDiarmid, A. G.; Chiang, C. K.; Heeger, A. J. *J. Chem. Soc. Chem. Commun.* **1977**, 578. (b) Chiang, C. K.; Fincher, C. R.; Park, Y. W.; Heeger, A. J.; Shirakawa, H.; Louis, E. J.; Gau, S. C.; MacDiarmid, A. G. *Phys. Rev. Lett.* **1977**, *39*, 1098.

(4) (a) Skotheim, T. A., Ed. In *Handbook of Conducting Polymers;* Marcel Dekker: New York, 1986. (b) Nalwa, H. S., Ed. In *Handbook of Organic Conductive Molecules and Polymers*; Wiley: New York, 1997. (c) Akagi, K.; Shirakawa, H. In *Electrical and Optical Polymer Systems: Fundamentals, Methods, and Applications*; Wise, D. L., Wnek, G. E., Trantolo, D. J., Cooper, T. M., Gresser, J. D., Eds.; Marcel Dekker: New York, 1998; Chapter 28, p 983.

(5) (a) Shirakawa, H.; Ikeda, S. *Polym. J.* **1971**, *2*, 231. (b) Tanabe, Y.; Kyotani, H.; Akagi, K.; Shirakawa, H. *Macromolecules* **1995**, *28*, 4173.

(6) For instance: Shirakawa, H.; Masuda, T.; Takeda, T. In *The Chemistry of Triple-Bonded Functional Groups*, Suppl. C2; Patai, S., Ed.; Wiley: Chichester, U.K., 1994; Vol. 2, Chapter17.

(7) (a) Naarrmann, H.; Theophilou, N. *Synth. Met.* **1987**, *22*, 1. (b) Akagi, K.; Suezaki, M.; Shirakawa, H.; Kyotani, H.; Shimomura, M.; Tanabe, Y. *Synth. Met.* **1989**, *28*, D1. (c) Tsukamoto, J.; Takahashi, A.; Kawasaki, K. *Jpn. J. Appl. Phys.* **1990**, *29*, 125. (d) Cao, Y.; Smith, P.; Heeger, A. J. *Polymer* **1991**, *32*, 1210.

(8) (a) Shibahara, S.; Yamane, M.; Ishikawa, K.; Takezoe, H. *Macromolecules* **1998**, *31*, 3756. (b) Scherman, O. A.; Grubbs, R. H. *Synth. Met.* **2001**, *124*, 431. (c) Scherman, O. A.; Rutenberg, I. M.; Grubbs, R. H. *J. Am. Chem. Soc.* **2003**, *125*, 8515. (d) Schuehler, D. E.; Williams, J. E.; Sponsler, M. B. *Macromolecules* **2004**, *37*, 6255. (e) Gu, H.; Zheng, R.; Zhang, X.; Xu, B. *Adv. Mater.* **2004**, *16*, 1356.

(9) (a) Oh, S. Y.; Akagi, K.; Shirakawa, H.; Araya, K. *Macromolecules* **1993**, *26*, 6203. (b) Oh, S. Y.; Ezaki, R.; Akagi, K.; Shirakawa, H. *J. Polym. Sci., Part A : Polym. Chem.* **1993**, *31*, 2977. (c) Akagi, K.; Shirakawa, H. *Macromol. Symp.* **1996**, *104*, 137. (d) Kuroda, H.; Goto, H.; Akagi, K.; Kawaguchi, A. *Macromolecules* **2002**, *35*, 1307. (d) Goto, H.; Dai, X.; Ueoka, T.; Akagi, K. *Macromolecules* **2004**, *37*, 4783.

(10) (a) Jin, S. H.; Choi, S. J.; Ahn, W.; Cho, H. N.; Choi, S. K. *Macromolecules* **1993**, *26*, 1487. (b) Choi, S. K.; Gal, Y. S.; Jin, S. H.; Kim, H. K. *Chem. Rev.* **2000**, *100*, 1645. (c) Tang, B. Z.; Kong, X.; Wan, X.; Peng, H.; Lam, W. Y.; Feng, X. D.; Kwok, H. S. *Macromolecules* **1998**, *31*, 2419. (d) Kong, X.; Lam, J. W. Y.; Tang, B. Z. *Macromolecules* **1999**, *32*, 1722. (e) Geng, J.; Zhao, X.; Zhou, E.; Li, G.; Lam, J. W. Y.; Tang, B. Z. *Polymer* **2003**, *44*, 8095.

(11) (a) Koltzenburg, S.; Wolff, D.; Stelzer, F.; Springer, J.; Nuyken, O. *Macromolecules* **1998**, *31*, 9166. (b) Ting, C. H.; Chen, J. T.; Hsu, C. S. *Macromolecules* **2002**, *35*, 1180. (c) Schenning, A. P. H. J.; Fransen, M.; Meijer, E. W. *Macromol. Rapid Commun.* **2002**, *23*, 265. (d) Stagnaro, P.; Conzatti, L.; Costa, G.; Gallot, B.; Valenti, B. *Polymer* **2003**, *44*, 4443.

Recently, we have succeeded in synthesizing helical polyacetylene films through polymerization of acetylene under chiral nematic liquid crystal (N*-LC) used as an asymmetric reaction field.[14] The helical polyacetylene films consist of clockwise or counterclockwise helical structure of fibrils, which are the bundles of polyene chains. Helical polyacetylene is anticipated to show novel electromagnetic and optical properties,[14,15] and these properties are considered to depend on the screw degree of the fibrils. The morphology and the screw degree of the fibrils of helical polyacetylene is determined by the helical pitch of the N*-LC.

An N*-LC is prepared by adding a small amount of chiral dopant into nematic LC. The helical pitch (p) of the N*-LC can be adjusted by two methods: changing the twisting power or changing the concentration of the chiral dopant.[16] However, the mesophase temperature region of the N*-LC may also be affected by changing the concentration of the chiral dopant, which often becomes narrow as the concentration increases, and finally the mesophase will be destroyed when the concentration is close to a critical value.[17]

Addressing the limitation of the concentration method, we demonstrate herein an approach of utilizing chiral dopants with large twisting power for helical polyacetylene synthesis. Axially chiral binaphthyl derivatives have been reported to possess larger twisting powers than the compounds having asymmetric carbon atoms. Meanwhile, crown ethers are well-known to have the ability of forming a complex with an alkali, alkaline earth, or primary ammonium cation.[18] This interaction between crown ether and cation is named a host−guest effect.[19] Here we synthesized a series of crown ether type binaphthyl derivatives (CEBDs), in which one or two binaphthyl moieties were linked to a crown ether, with LC substituents being introduced to the 6,6′-positions of the binaphthyl moiety. The aim is to control the twisting power of the CEBDs for the nematic LC, by optimizing the ring size of the crown ether. Besides, the twisting powers of the CEBDs might be controlled through the host−guest interaction between the crown ether and a cation.

The target of this research is to control the helical pitch of N*-LCs by changing the twisting power of the CEBDs, through which the morphology of the helical polyacetylene can be controlled.

Scheme 1. Crown Ether Type Binaphthyl Derivatives (CEBDs)

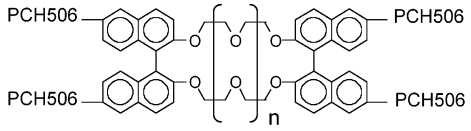

R-**1**, *S*-**1** (*n* = 1)
R-**2**, *S*-**2** (*n* = 2)
R-**3**, *S*-**3** (*n* = 3)

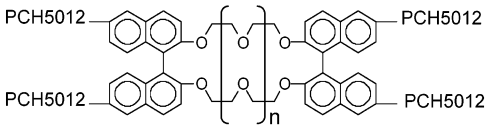

R-**4**, *S*-**4** (*n* = 1)
R-**5**, *S*-**5** (*n* = 2)

di-substituted CEBDs

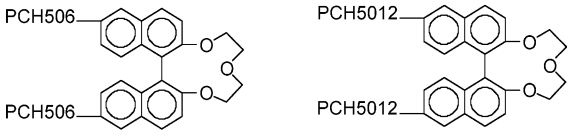

R-**6** *R*-**7**

mono-substituted CEBDs

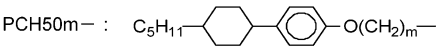

(*m* = 6, 12)

2. Methods

2.1. Synthesis of CEBDs. Two types of CEBDs, monosubstituted and disubstituted CEBDs, were synthesized, in which one and two binaphthyl moieties were linked to crown ether, respectively. Their molecular structures were shown in Scheme 1. To improve their miscibility with the phenylcyclohexane (PCH)-derived nematic LCs used for acetylene polymerization, LC substituents having PCH mesogen core were introduced to the 6,6′-positions of the binaphthyl group. For the investigation of the effect of methylene spacer length in the LC substituents on the twisting powers of the CEBDs, two kinds of methylene spacers (m = 6, 12) were designed. Their synthesis method is shown in Scheme 2.

Proton (^{1}H) and carbon (^{13}C) nuclear magnetic resonance (NMR) spectra were measured in $CDCl_3$ using a JEOL 270 MHz NMR spectrometer. Chemical shifts are represented in parts per million downfield from tetramethylsilane as an internal standard. Infrared spectra were measured using a JASCO FT-IR 550 spectrometer. The chemical and physical properties of the compounds synthesized are given in the last section.

2.2. Preparation of N*-LC. An N*-LC was prepared by adding a small amount (0.5 mol %) of CEBD, as a chiral dopant, into an equimolar mixture of the nematic LCs of phenylcyclohexane derivatives, 4-(*trans*-4-*n*-propylcyclohexyl)ethoxybenzene (PCH302) and 4-(*trans*-4-*n*- propylcyclohexyl)butoxybenzene (PCH304). It should be noted that although each component (PCH302 or PCH304) shows a LC phase, the LC temperature region is very narrow, i.e., less than 1−2 °C. This is not suitable for acetylene polymerization in a nematic or chiral nematic LC reaction field, because the exothermal heat evoked during the acetylene polymerization would raise the temperature inside a Schlenk flask and easily destroy the LC phase into an isotropic one. Hence, we prepared a LC mixture by mixing equimolar two LC components. In the LC mixture, the nematic−isotropic temperature, T_{N-I}, and the crystalline−nematic temperature, T_{C-N}, might be raised

(12) (a) Araya, K.; Mukoh, A.; Narahara, T.; Shirakawa, H. *Synth. Met.* **1986**, *4*, 199. (b) Akagi, K.; Shirakawa, H.; Araya, K.; Mukoh, A.; Narahara, T. *Polym. J.* **1987**, *19*, 185. (c) Akagi, K.; Katayama, S.; Shirakawa, H.; Araya, K.; Mukoh, A.; Narahara, T. *Synth. Met.* **1987**, *17*, 241. (d) Akagi, K.; Katayama, S.; Ito, M.; Shirakawa, H.; Araya, K. *Synth. Met.* **1989**, *28*, D51. (e) Sinclair, M.; Moses, D.; Akagi, K.; Heeger, A. J. *Phys. Rev. B: Condens. Matter* **1988**, *38*, 10724.
(13) (a) Montaner, A.; Rolland, M.; Sauvajol, J. L.; Galtier, M.; Almairac, R.; Ribet, J. L. *Polymer* **1988**, *29*, 1101. (b) Coustel, N.; Foxonet, N.; Ribet, J. L.; Bernier, P.; Fischer, J. E. *Macromolecules* **1991**, *24*, 5867.
(14) (a) Akagi, K.; Piao, G.; Kaneko, S.; Sakamaki, K.; Shirakawa, H.; Kyotani, M. *Science* **1998**, *282*, 1683. (b) Akagi, K.; Piao, G.; Kaneko, S.; Higuchi, I.; Shirakawa, H.; Kyotani, M. *Synth. Met.* **1999**, *102*, 1406. (c) Akagi, K.; Higuchi, I.; Piao, G.; Shirakawa, H.; Kyotani, M. *Mol. Cryst. Liq. Cryst.* **1999**, *332*, 463.
(15) (a) Suh, D. S.; Kim, T. J.; Aleshin, A. N.; Park, Y. W.; Piao, G.; Akagi, K.; Shirakawa, H.; Qualls, J. S.; Han, S. Y.; Brooks, J. S. *J. Chem. Phys.* **2001**, *114*, 7222. (b) Aleshin, A. N.; Lee, H. J.; Park, Y. W.; Akagi, K. *Phys. Rev. Lett.* **2004**, *93*, 196601. (c) Lee, H. J.; Jin, Z. X.; Aleshin, A. N.; Lee, J. Y.; Goh, M. J.; Akagi, K.; Kim, Y. S.; Kim, D. W.; Park, Y. W. *J. Am. Chem. Soc.* **2004**, *126*, 16722.
(16) Gottarelli, G.; Mariani, P.; Spada, G. P.; Samori, B.; Forni, A.; Solladie, G.; Hibert, M. *Tetrahedron* **1983**, *39*, 1337.
(17) (a) Semenkova, G. P.; Kutulya, L. A.; Shkol'nikova, N. I.; Khandrimailova, T. V. *Kristallografiya* **2001**, *46*, 128. (b) Guan, L.; Zhao, Y. *J. Mater. Chem.* **2001**, *11*, 1339. (c) Hatoh, H. *Mol. Cryst. Liq. Cryst. Sci. Technol., Sect. A* **1994**, *250*, 1. (d) Lee, H.; Labes, M. M. *Mol. Cryst. Liq. Cryst.* **1982**, *84*, 137.
(18) Pederson, C. J. *J. Am. Chem. Soc.* **1967**, *89*, 2495, 7017.
(19) Kuhn, R.; Erni, F. *Anal. Chem.* **1992**, *64*, 2815.

Scheme 2. Synthetic Routes for CEBDs

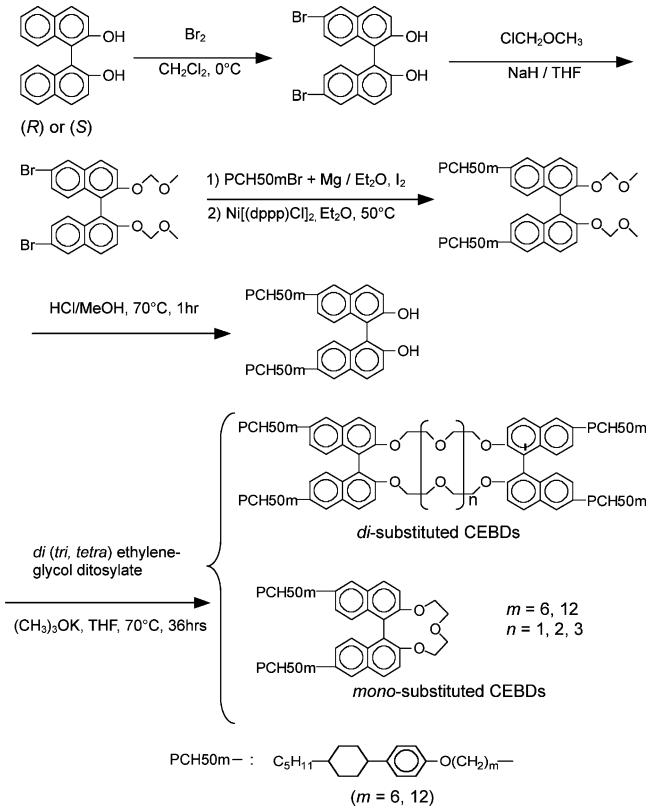

and lowered, respectively. In fact, the mixture exhibited the LC phase in the region from 20 to 35 °C. Subsequently, the change of T_{N-I} upon an addition of Ti(O-*n*-Bu)$_4$−AlEt$_3$ catalyst was examined through DSC measurement. Taking account of the effect of supercooling for LCs, the catalyst solution consisting of the LC mixture and the chiral dopant was found available for room-temperature polymerization ranging form 5 to 25 °C. This sufficiently wide temperature region enabled us to perform the acetylene polymerization in the N*-LC phase.

2.3. Measurements of Helical Pitch and Twisting Power. The helical pitch of the N*-LC was evaluated with Cano's wedge method,[20] using a polarized optical microscope under temperature control (heating and cooling rate of 10 °C/min). The microscope observation was carried out under crossed nicols by using a Nikon ECLIPSE E 400 POL polarizing optical microscope equipped with a Nikon COOLPIX 950 digital camera and a Linkam TH-600PM and L-600 heating and cooling stage with temperature control.

The Cano's wedge method is schematically described in Scheme 3. When the N*-LC sample was inserted into a wedge-type cell with gradient thickness, the discontinuity lines named Cano lines appeared on the surface of the cell under crossed nicols.[20−22] The helical pitch (p) was evaluated by measuring the distance (a) between Cano lines as follows:

$$p = 2a \tan \theta$$

where θ is the angle of the wedge of the cell. The twisting power (β_M) of the chiral dopant was evaluated with the following equation:[20]

$$\beta_M = 1/(pcr)$$

where c is the molar concentration of the chiral dopant and r is the enantiometric purity of the chiral dopant; here, r is assumed to be 1. The concentration of the chiral dopant was 5 mmol %, where the concentrations of PCH302 and PCH304 and the chiral dopant were 100:100:1 in molar ratio.

2.4. Polymerization of Acetylene. The N*-LC was used as solvent for the Ziegler−Natta catalyst consisting of Ti(O-*n*-Bu)$_4$ and AlEt$_3$. The concentration of [Ti] was 20 mmol/L, and the mole ratio of the cocatalyst to catalyst [Al]/[Ti] was 4.0. The catalyst solution was aged for 30 min at room temperature, then was completely degassed through a vacuum line, and was transferred into a flat-bottomed container inside a Schlenk flask. The polymerization was carried out by introducing acetylene gas into the catalyst solution. The polymerization temperature was kept at 16 to ~18 °C to maintain the N* phase. The initial acetylene pressure was about 30 torr; the polymerization was stopped when the pressure decreased by 5 torr. The polyacetylene film thus obtained was washed with purified toluene/methanol solution containing 1 N hydrochloric acid and THF in turns, and was dried through vacuum line on a Teflon sheet for 2 h. The thickness of the films was from 4 to 8 μm.

3. Results and Discussion

3.1. Twisting Power and Specific Rotation of CEBDs. The twisting powers (β_M) of CEBDs were evaluated with Cano's wedge method,[20] which was based on the observation of discontinuity lines that appeared when a N*-LC was inserted into a cell with a gradient thickness. Table 1 shows the variation of twisting powers of the CEBDs having *R* configuration with their structures.

As shown in Table 1, the twisting power (β_M) increased with the decrease of the ring size of the crown ether for disubstituted CEBDs (*R*-**1**, *R*-**2**, and *R*-**3**). The ring size of the crown ether is here expressed with the number of oxydimethylene repeat units (n) in the crown ether. Disubstituted CEBDs (*R*-**1**, *R*-**4**) showed larger twisting power than monosubstituted ones having the same substituent (*R*-**6**, *R*-**7**). For both mono- and disubstituted CEBDs, the shorter the methylene spacer (m) in the LC substituents, the larger the twisting power (*R*-**1** and *R*-**4**, *R*-**2** and *R*- **5**, *R*-**6** and *R*-**7**).

Besides the twisting power, the specific rotation ([α]$^{23}_D$) can also be used to characterize optical activity of a chiral compound.[21] To investigate the relationship between twisting power and specific rotation, we also measured the specific rotation for the CEBDs at 23 °C. The results are shown in the fourth column of Table 1. For disubstituted CEBDs, the specific rotation increased with decreasing ring size of the crown ether. It also tends to increase with shortening of the methylene spacer (m) in the LC substitution of the biphenyl moiety. A similar tendency seems to be seen in the cases of monosubstituted CEBDs. Note that although the twisting power of monosubstituted CEBD *R*-**7** is about one-third of that of disubstituted CEBD *R*-**4**, the specific rotation of *R*-**7** is comparable to that of *R*-**4** in absolute value. A similar situation can be seen between monosubstituted CEBD *R*-**6** and disubstituted CEBD *R*-**1**. This implies that the twisting powers of the CEBDs have no direct relationship with their specific rotations.[22] Nevertheless, one may remark that the relatively small size of CEBD is suitable for generating large specific rotation and/or twisting power.

It is interesting to note that the monosubstituted and disubstituted CEBDs having the same *R* configuration show different

(20) (a) Gottarelli, G.; Samori, B.; Stremmenos, C.; Torre, G. *Tetrahedron* **1981**, *37*, 395. (b) Grandjean, F. *C. R. Acad. Sci.* **1921**, 172. (c) Cano, R. *Bull. Soc. Fr. Mineral.* **1968**, *91*, 20.
(21) Morrison, R. T.; Boyd, R. N. In *Organic Chemistry* (5th ed.); Tokyo Kagaku Dojin: Tokyo, 1989; pp 164−166.
(22) (a) Finkelmann, H.; Stegemeger, H. *Z. Naturforsch., A: Phys. Sci.* **1973**, *28*, 799. (b) Finkelmann, H.; Stegemeger, H. *Ber. Bunsen-Ges. Phys. Chem.* **1978**, *82*, 1302.

Scheme 3. Cano's Wedge Method for the Helical Pitch (p) and Twisting Power (β_M) of the Chiral Dopant in N*-LC

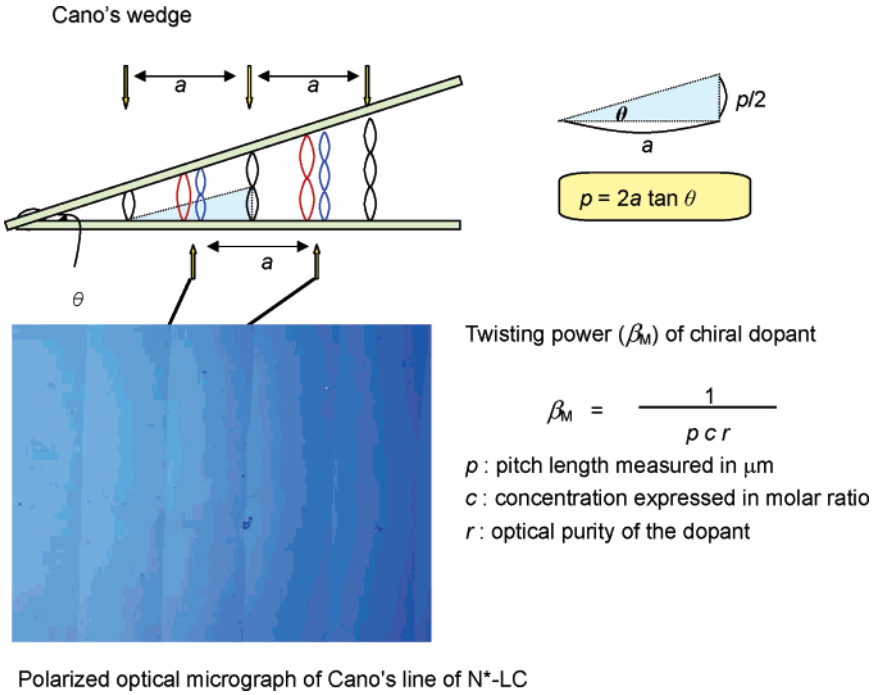

Table 1. Twisting Power (β_M) and Specific Rotation ($[\alpha]^{23}_D$) of CEBDs with the *R* Configuration, Helical Pitch, and Screw Direction of the Corresponding N*-LCs

CEBDs with *R configuration*					N*-LCs[a]	
type	n[b]	CEBD (methylene spacer)	$[\alpha]^{23}_D$	β_M (μm^{-1})[c]	helical pitch (μm)[c]	screw direction[d]
disubstituted CEBDs	1	*R*-**1** ($m = 6$)	+48.7	64.3	3.1	right-handed
	2	*R*-**2** ($m = 6$)	+24.5	51.3	4.2	right-handed
	3	*R*-**3** ($m = 6$)	+15.3	15.4	13.0	right-handed
	1	*R*-**4** ($m = 12$)	+22.8	53.2	3.8	right-handed
	2	*R*-**5** ($m = 12$)	+7.5	35.0	5.7	right-handed
monosubstituted CEBDs	1	*R*-**6** ($m = 6$)	−39.1	20.6	9.7	left-handed
	1	*R*-**7** ($m = 12$)	−25.0	16.1	12.4	left-handed

[a] Composed of PCH302, PCH304, and chiral dopant with the mole ratio of 100:100:1. [b] The variable n is the number of oxydimethylene repeat units in the crown ether. [c] Measured with Cano's wedge method at room temperature (see Scheme 3). [d] Determined with a miscibility test, in which cholesteryl oleyl carbonate is used as the standard N*-LC.

signs in specific rotation: the former is a negative value while the latter is a positive value. This implies that these two kinds of CEBDs have different screw directions. In fact, it is confirmed by the miscibility test that the N*-LCs induced by the mono- and disubstituted CEBDs exhibit different screw directions, i.e., left-handed and right-handed ones, respectively, as shown in Table 1. Before the above result is discussed, it is helpful to remember that (*R*)-(+)-1,1′-bi-2-naphthol and (*R*)-(−)-1,1′-binaphthyl-2,2′-diyl-hydrogenphosphate are dextro-rotatory (+) and levo-rotatory (−), respectively, despite having the same (*R*) configuration.[23] The latter has a bridged structure linking two oxygen atoms at the 2,2′-positions of the binaphthyl rings via a −P(O)(OH) moiety (see Scheme 4).

This implies that the axial chirality of the binaphthyl derivative sensitively depends on the local structure around the 2,2′-positions of the binaphthyl rings, as well as on the change of the dihedral angle defined by the two binaphthyl rings. This

(23) Jacques, J.; Fouquey, C. *Org. Synth.* **1989**, *67*, 1.

Scheme 4. (*R*)-(+)-1,1′-Bi-2-naphthol (Left) and (*R*)-(−)-1,1′-Binaphthyl-2,2′-diyl-hydrogenphosphate (Right)

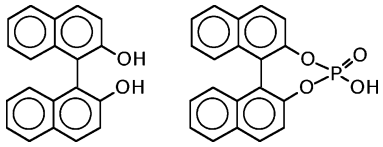

situation is similar to the present case where the mono- and disubstituted CEBDs with the same (*R*) configuration give an opposite sign in specific rotation. It is expected that the larger crown ether type cyclic ring of the disubstituted CEBD, compared with that of the monosubstituted CEBD, might lead to more flexibility in the dihedral angle. Although the specific rotation (specific rotatory power) is determined by the scalar product of the transition electric dipole moment and the magnetic dipole moment, it is difficult here to argue how both the bridged structure and the change of the dihedral angle affect the sign of specific rotation, requiring rigorous theoretical calculations.

The twisting power of the CEBDs may also be affected by temperature, and the affecting degree depends on the ring size of the crown ether (Figure 1). The twisting power of *R*-**1,** which has the smallest crown ether ring size ($n = 1$), decreased from 78 to 63 μm^{-1} when the temperature increased from 10 to 32

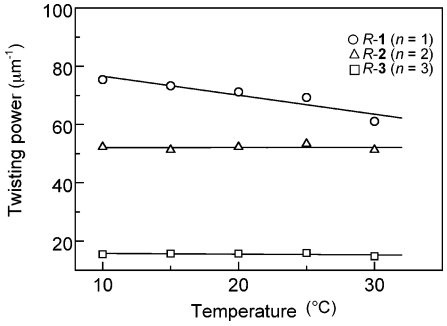

Figure 1. Effect of temperature on the twisting power of CEBDs.

Table 2. Changes of Twisting Powers (β_M) of Disubstituted Crown Ether Type Binaphthyl Derivatives (CEBDs) after Addition of $CuCl_2$

		twisting powers, β_M (cm^{-1})[a]		
n[b]	disubstituted CEBDs	before addition of $CuCl_2$	after addition of $CuCl_2$	$\Delta\beta_M$ (cm^{-1})[c]
1	*R*-**1**	64.3	58.1	−6.2
	S-**1**	65.1	58.3	−6.8
2	*R*-**2**	51.3	47.2	−4.1
	S-**2**	52.0	47.5	−4.5
3	*R*-**3**	15.4	11.3	−4.1
	S-**3**	15.5	11.5	−4.0

[a] Measured with Cano's wedge methods at room temperature (see Scheme 3). [b] The variable n is the number of oxydimethylene repeat units in the crown ether. [c] Difference in twisting power before and after addition of $CuCl_2$.

°C. On the other hand, the twisting powers of *R*-**2** and *R*-**3**, which have larger crown ether ring sizes (n = 2 and 3), almost did not change with temperature. Because the helical pitch of a N*-LC is inversely proportional to the twisting power of a chiral dopant,[16] it can be deduced that the helical pitch of the N*-LC induced by *R*-**1** will be shortened with decreasing temperature. That is to say, we should set the acetylene polymerization temperature at the lower side of the mesophase temperature region for the N*-LC to improve the screw degree of the polyacetylene fibrils. But for the N*-LCs induced by *R*-**2** and *R*-**3**, the polymerization temperature can be set at any point in the mesophase temperature region, because the helical pitch will almost not change with temperature.

It is well-known that the conformation of the crown ether can be changed by adding a cation with suitable size (e.g., K^+, Cu^{2+}) into its solution. The twisting power of the CEBDs may be controlled through this conformational change of the crown ether. Here we examined the host−guest reactivity of $CuCl_2$ with the CEBDs. When $CuCl_2$ was added into the $CHCl_3$ solution of the CEBDs, the color of the solution changed from colorless to red. The differential scanning calorimeter (DSC) results showed that the original peaks of the CEBDs disappeared, while new peaks appeared with the addition of $CuCl_2$. Meanwhile, the ^1H NMR spectra showed that the peaks derived from the chemical shifts of protons in the crown ether broadened with the addition of $CuCl_2$. These results implied the formation of a host−guest complex between the crown ether and Cu^{2+}. As shown in Table 2, the twisting powers of the disubstituted CEBDs decreased slightly by 4 to 6 μm^{-1} after the complex formation with $CuCl_2$.

It is likely that the degree of decrease in the twisting power is larger in the CEBD with a smaller crown ether ring size. This suggests that the complex formation tends to weaken the axial chirality of the CEBD by depressing the twisting of the binaphthyl dihedral angle and that this is more effective in the CEBD with a smaller crown ether ring size. One may remark that the twisting power of the CEBDs can be adjusted to some extent through the host−guest interaction between the crown ether and the cation.

3.2. Helical Pitch and Screw Direction of N*-LCs. As shown in Table 1, the helical pitch of N*-LCs induced by CEBDs varied from 3.0 to 13.1 μm upon changing the ring size of the crown ether, methylene spacer, and the number of binaphthyl moieties. The helical pitch of the N*-LC induced by *R*-**1**, which is the shortest one in this research, further

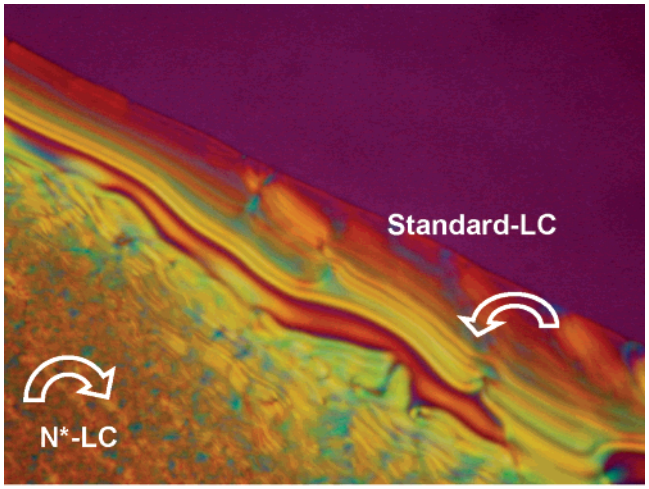

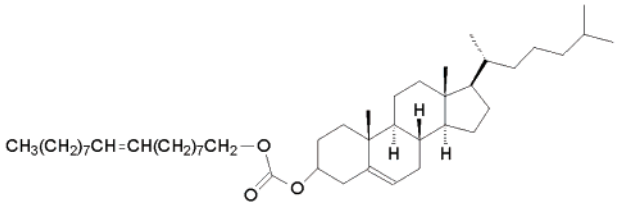

Standard LC: Cholesteryl Oleyl Carbonate

Figure 2. Miscibility test for screw direction of the N*-LC induced by *R*-**2**.

decreased from 3.2 to 2.6 μm when the temperature decreased from 32 to 10 °C. In this way, the N*-LC with the shortest helical pitch could be obtained.

The screw directions of the N*-LCs induced by the CEBDs were determined through the miscibility test method.[24] This method is based on the observation of the mixing area between a N*-LC and a standard LC through a polarized optical microscope (POM), in which the screw direction of the standard LC is known. If the screw direction of the N*-LC is the same as that of the standard LC, the mixing area will be continuous. Otherwise, it will be discontinuous (shown as a Schlieren texture of the nematic LC). Figure 2 gives the POM image of the mixture of the N*-LC induced by *R*-**2** and a standard LC of cholesteryl oleyl carbonate (left-handed). As shown in the figure, there appeared a discontinuous area between the N*-LC and the standard LC. Because the screw direction of the standard LC is known to be left-handed, the screw direction of the N*-LC induced by *R*-**2** can thus be deduced to be opposite to that of the standard LC, i.e., right-handed.

The screw direction of the N*-LCs induced by disubstituted and monosubstituted CEBDs are listed in the last column of Table 1. The N*-LCs induced by disubstituted CEBDs having *R* configuration all showed right-handed helical structure, but those induced by monosubstituted CEBDs having the same *R* configuration showed left-handed helical structure. These results coincided with the opposite signs in the specific rotation of these two kinds of CEBDs (the fourth row in Table 1).

3.3. Morphology of Helical Polyacetylene. Using the disubstituted CEBDs of *R*-**1**, *R*-**2**, and *R*-**3** for the induction of

(24) Uchida, T.; Inukai, T. In *Liquid Crystal-Fundamentals*; Okano, K., Kobayashi, S., Eds.; Baifukan: Tokyo, 1985; p 205−231.

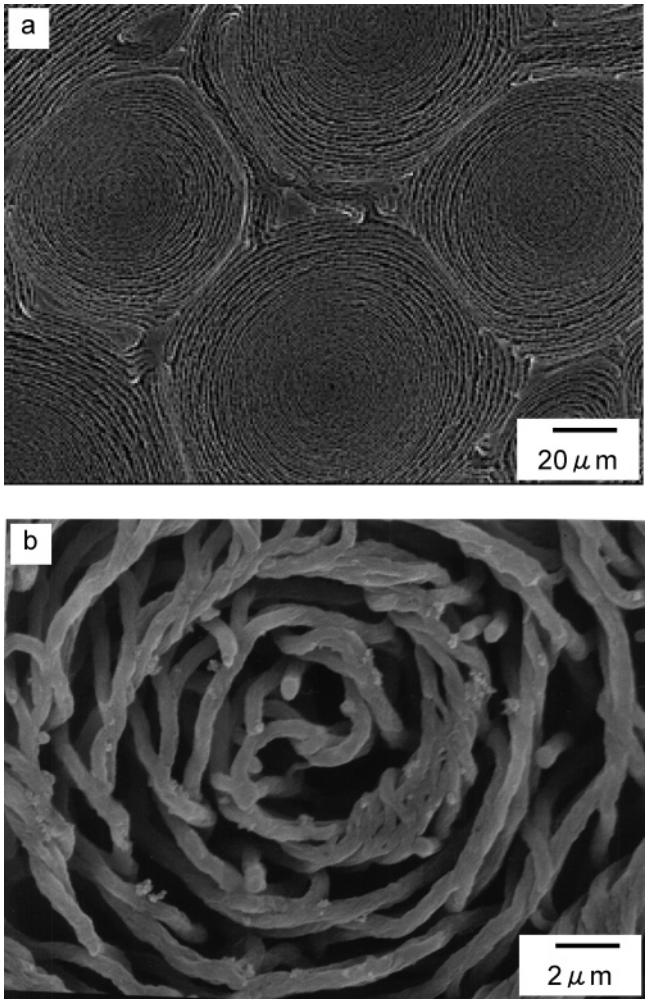

Figure 3. SEM images of the helical polyacetylene synthesized in the N*-LC induced by *R*-**2**; (b) is the magnified image of (a).

N*-LCs, and the thus-obtained N*-LCs as the reaction field for acetylene polymerization, we have successfully synthesized polyacetylene films with helical morphology. Note that we did not get enough amounts of *R*-**4**−*R*-**7** to carry out the polymerization reaction, owing to their low reaction yields. Figure 3 shows scanning electron microscopic (SEM) photographs of polyacetylene film synthesized under a N*-LC induced by *R*-**2**. As shown in Figure 3, there existed many spiral domains in the film, and the fibrils screwed in a counterclockwise direction to form a bundle, and the bundle screwed in the same direction to form the spiral domain.

We then investigated the parameters (such as the interdistance between the fibril bundles, and the diameter of a fibril bundle and that of a fibril) of these helical polyacetylenes through the magnified SEM images. The parameters of the helical polyacetylenes synthesized in the N*-LCs induced by *R*-**1**, *R*-**2**, and *R*-**3** are summarized in Table 3. The interdistance between the fibril bundles of helical polyacetylene decreased with increasing twisting power of the CEBDs (decrease of helical pitch of the N*-LC); all equaled about a half-helical pitch of the corresponding N*-LCs. Although the diameter of the fibril bundles decreased with increasing twisting power of the CEBDs, that of a fibril did not change, being in the range of 120−130 nm.

For helical polyacetylenes synthesized in the N*-LCs induced by disubstituted CEBDs having *R* configuration, *R*-**1**−*R*-**3**, the fibrils screwed in a counterclockwise direction (left-handed), but the miscibility test has shown that N*-LCs induced by these CEBDs have right-handed helical structure (the last column of Table 1), from which we can get an interesting result that the screw direction of the fibrils of helical polyacetylene is opposite to that of the N*-LC used as the polymerization solvent. This is an unexpected and even surprising result, requiring a sound interpretation. It has been elucidated so far that the polyacetylene chains propagate along the director (an averaged direction for the LC molecules within a domain) of the N*-LC. Since the helical axis of polyacetylene is parallel to the polyacetylene chain, and the director of the N*-LC is perpendicular to the helical axis of N*-LC, the helical axis of polyacetylene is perpendicular to that of the N*-LC. Taking into account these aspects, we described a plausible mechanism for interfacial acetylene polymerization in N*-LC, as shown in Figure 4. In the case of a right-handed N*-LC, for instance, the polyacetylene chain would propagate with a left-handed manner, starting from the catalytic species, but not with a right-handed one. This is because the polyacetylene chains with the opposite screw direction to that of the N*-LC could propagate along the LC molecules, but those with the same direction as that of the N*-LC would encounter LC molecules, making the propagation stereospecifically impossible. The detailed mechanism of acetylene polymerization in N*-LC is now under investigation and will be discussed elsewhere.

Table 3. Parameters of Helical PAs Synthesized in N*-LCs Induced by Disubstituted CEBDs with *R*-Configuration

chiral dopant		N*-LC	helical PA		
CEBD	twisting power (μm^{-1})	helical pitch (μm)	interdistance between fibril bundles (±0.2 μm)	diameter of a fibril bundle (±0.2 μm)	diameter of a fibril (±20 nm)
R-**1**	64.3	3.1	1.6	0.5	120
R-**2**	51.3	4.2	2.0	0.6	120
R-**3**	15.4	13.0	7.0	2.5	130

Based on the results above, we can summarize the relationship between the morphology of helical polyacetylene and the helical structure of the N*-LC used as the polymerization solvent, i.e., the interdistance between the fibril bundles of the helical polyacetylene is equal to about a half-helical pitch of the N*-LC, and the screw direction of the polyacetylene fibrils is opposite to that of the N*-LC. These results are very important hints for clarifying the formation mechanism of helical polyacetylene in the asymmetric reaction field of N*-LC.

Helical polyacetylene films synthesized in this research were trans-rich polymers, because a relatively high polymerization temperature from 16 to 18 °C was adopted to maintain the N* phase. The electrical conductivities of the films were in the range from 1.5×10^3 to 2.0×10^3 S/cm after iodine doping. With so high a value of electrical conductivity, helical polyacetylene has become one of the most prospective electrically conductive polymers for application. Research on helical structure control and application of helical polyacetylene are ongoing.

4. Conclusion

By investigating twisting power of a series of CEBDs and by comparing the morphology of helical polyacetylenes synthesized in N*-LCs induced by the CEBDs, it was found that the twisting power of the CEBDs increased with decreasing ring size of the crown ether. With increasing twisting power of the

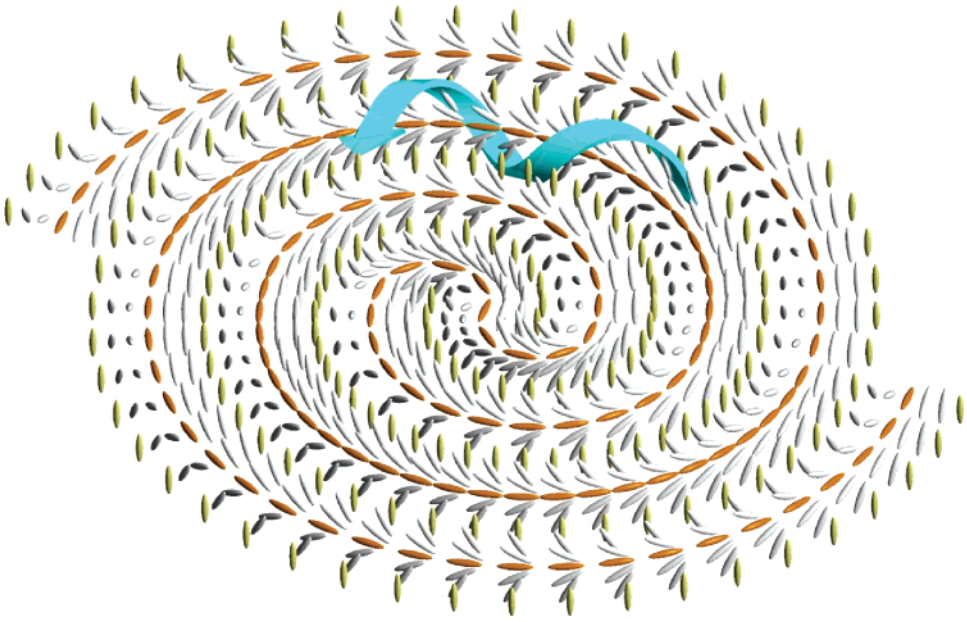

Figure 4. Schematic representation of the propagation of helical polyacetylene in the chiral nematic liquid crystal (N*-LC). The helical polyacetylene with the left-handed screw direction (blue arrow) grows up starting from the catalytic species in a right-handed N*-L.

CEBDs, the interdistance between the fibril bundles of the helical polyacetylene decreased, the diameter of a fibril bundle decreased, but the diameter of a fibril did not change. The interdistance between the fibril bundles of the helical polyacetylene equaled about a half-helical pitch of the N*-LC, and the screw direction of the polyacetylene fibrils was opposite to that of the N*-LC.

Last it is worth noting that very recently, besides helical polyacetylene, other kinds of spiral morphology containing conjugated polymers such as polythiophene, polypyrrole, and polyethylenedioxythiophne derivatives have also been synthesized through chemical or electrochemical polymerization in N*-LC using ordinary chiral binaphthyl derivatives.[25] Therefore, the present CEBDs should be promising chiral dopants to control more precisely the screwed structures of these conjugated polymers, by virtue of the ring size effect of the crown ether and the host−guest interaction.

5. Experimental Section

5.1. (*R*)-Crown(2)-(6,6′-PCH506-Binol)$_2$ (*R*-1). ^{1}H NMR ($CDCl_3$, δ from TMS, ppm): 0.86−1.87 (m, 112H, $-CH_3$, $-CH_2-$, cyclohexyl−H), 2.39 (t, 4H, J = 12.0, Ph−cyclohexyl−H), 2.70 (t, J = 7.6, Ar−CH_{2-}), 3.17−3.37 (m, 8H, crown ether ($-CH_2$)), 3.80−3.91 (m, 8H, crown ether (CH_2)), 3.91 (t, 8H, J = 6.5, $-CH_2O-$Ph), 6.80 (dd, 8H, J = 8.6, 2.8, O−Ph−H), 7.01 (s, 8H, cyclohexyl−Ph−H), 7.09 (d, 8H, J = 8.7, Ar−H (3,3′,7,7′)), 7.27 (d, 4H, J = 11.7, Ar−H (4,4′)), 7.62 (s, 4H, Ar−H (5,5′)), 7.85 (d, 4H, J = 9.1, Ar−H (8,8′)). ^{13}C NMR ($CDCl_3$, δ from TMS, ppm): 14.12, 22.72, 25.97, 26.67, 27.31, 29.14, 29.29, 31.22, 32.23, 33.68, 34.59, 35.75, 37.33, 37.41, 43.74, 54.80, 67.87, 69.21, 69.47, 72.48, 102.20, 114.24, 115.67, 118.05, 120.64, 126.08, 126.75, 127.57, 127.84, 128.52, 129.52, 132.64, 137.83, 139.93, 153.59, 157.20, 169.82. FT-IR (KBr, cm^{-1}): 2923.6(s), 2856.1(s), 1594.8(m), 1511.9(s), 1456.0(w), 1246.7(s), 1175.8(w), 1095.4(w), 825.4(m), 543.8(w), 461.3(w). Anal. Calcd for $C_{140}H_{184}O_{10}$: C, 82.96; H, 9.15. Found: C, 82.68; H, 9.15.

5.2. (*R*)-Crown(3)-(6,6′-PCH506-Binol)$_2$ (*R*-2). ^{1}H NMR ($CDCl_3$, δ from TMS, ppm): 0.86−1.86 (m, 112H, $-CH_3$, $-CH_2-$, cyclohexyl−H), 2.39 (t, 4H, J = 12.1, Ph−cyclohexyl−H), 2.70 (t, 8H, J = 7.6, Ar−CH_{2-}), 3.18 (s, 8H, crown ether (CH_2)), 3.35−3.46 (m, 8H, crown ether (CH_2)), 3.91 (t, 8H, J = 6.4, Ph-OCH_{2-}), 3.88−4.08 (m, 8H, crown ether (CH_2)), 6.80 (d, 8H, J = 8.7, O−Ph−H), 7.03−7.11 (m, 16H, cyclohexyl−Ph−H, Ar−H (3,3′,7,7′)), 7.40 (d, 4H, J = 8.9, Ar−H (4,4′), 7.61 (s, 4H, Ar−H (5,5′)), 7.84 (d, 4H, J = 9.1, Ar−H (8,8′)). ^{13}C NMR ($CDCl_3$, δ from TMS, ppm): 14.13, 22.72, 25.98, 26.67, 29.14, 29.30, 31.22, 32.23, 33.67, 34.59, 35.76, 37.31, 37.41, 43.73, 67.86, 69.76, 69.88, 70.51, 114.22, 116.48, 120.91, 125.48, 126.15, 127.37, 127.57, 127.83, 128.61, 129.66, 132.55, 137.91, 139.93, 153.91, 157.18. FT-IR (KBr, cm^{-1}): 2925.5(s), 2854.1(s), 1594.8(m), 1511.9(s), 1456.0(w), 1245.8(s), 1095.4(w), 825.4(m), 543.8(w), 446.7(w). Anal. Calcd for $C_{144}H_{192}O_{12}$: C, 81.77; H, 9.15. Found: C, 81.18; H, 9.16.

5.3. (*R*)-Crown(4)-(6,6′-PCH506-Binol)$_2$ (*R*-3). ^{1}H NMR ($CDCl_3$, δ from TMS, ppm): 0.89−1.87 (m, 112H, $-CH_3$, $-CH_2-$, cyclohexyl−H), 2.39 (t, 4H, J = 12.3, Ph−cyclohexyl−H), 2.70 (t, 8H, J = 7.7, Ar−CH_{2-}), 3.21∼3.32 (m, 16H, crown ether (CH_2)), 3.32−3.53 (m, 16H, crown ether (CH_2)), 3.91 (t, 8H, J = 6.4, Ph−OCH_{2-}), 3.88−4.11 (m, 8H, crown ether ($-CH_{2-}$)), 6.80 (d, 8H, J = 8.8, O−Ph−H), 7.08 (t, 16H, J = 8.4, cyclohexyl−Ph−H, Ar−H (3,3′,7,7′)), 7.39 (d, 4H, J = 9.1, Ar−H (4,4′)), 7.60 (s, 4H, Ar−H (5,5′)), 7.83 (d, 4H, J = 9.1, Ar−H (8,8′)). ^{13}C NMR ($CDCl_3$, δ from TMS, ppm): 14.11, 21.62, 22.71, 25.96, 26.67, 29.15, 29.29, 31.22, 32.22, 33.66, 34.59, 35.48, 35.75, 37.30, 37.41, 43.73, 49.71, 67.85, 69.74, 70.03, 70.47, 70.62, 76.54, 112.79, 114.21, 116.19, 120.79, 125.49, 126.13, 127.56, 127.81, 127.97, 128.59, 129.60, 129.84, 132.53, 134.31, 137.88, 139.90, 153.87, 157.18, 164.20, 179.54, 188.72, 190.23. FT-IR (KBr, cm^{-1}): 2923.6(s), 2854.1(s), 1596.8(m), 1511.9(s), 1456.0(w), 1351.9(w), 1245.8(s), 1176.4(w), 1097.3(w), 825.4(m), 553.5(w). Anal. Calcd for $C_{148}H_{200}O_{14}$: C, 80.68; H, 9.15. Found: C, 79.98; H, 9.18.

5.4. (*R*)-Crown(2)-(6,6′-PCH5012-Binol)$_2$ (*R*-4). ^{1}H NMR ($CDCl_3$, δ from TMS, ppm): 0.86−1.87 (m, 160H, $-CH_3$, $-CH_{2-}$, cyclohexyl (CH_2)), 2.39 (t, 4H, J = 12.0, Ph−cyclohexyl−H), 2.68 (t, 8H, J = 7.6, Ar−CH_{2-}), 3.14−3.28 (m, 8H, crown ether (CH_2)), 3.79−3.93 (m, 8H, crown ether (CH_2)), 3.90 (t, 8H, Ph−OCH_{2-}), 6.81 (d, 8H, J = 8.7, O−Ph−H), 7.00 (m, 8H, cyclohexyl−Ph−H), 7.11 (d, 8H, J = 2.7, Ar−H (3,3′,7,7′)), 7.29 (s, 4H, Ar−H (4,4′)), 7.61 (s, 4H, Ar−H (5,5′)), 7.85 (d, 4H, J = 8.9, Ar−H (8,8′)).

(25) (a) Goto, H.; Akagi, K. *Macromolecules* **2005**, *38*, 1091. (b) Goto, H.; Akagi, K. *J. Polym. Soc, Part A: Polym. Chem.* **2005**, *43*, 616. (c) Goto, H.; Akagi, K. *Macromol. Rapid Commun.* **2004**, *25*, 1482. (d) Goto, H.; Jeong, Y. S.; Akagi, K. *Macromol. Rapid Commun.* **2005**, *26*, 164.

5.5. (*R*)-Crown(3)-(6,6′-PCH5012-Binol)$_2$ (*R*-5). ^{1}H NMR ($CDCl_3$, δ from TMS, ppm): 0.90∼1.90 (m, 160H, $-CH_3$, $-CH_{2-}$, cyclohexyl−H), 2.42 (t, 4H, J = 12.1, Ph−cyclohexyl−H), 2.67 (t, 8H, J = 7.6, Ar−CH_{2-}), 3.21 (s, 8H, crown ether (CH_2)), 3.21∼3.53 (m, 8H, crown ether (CH_2)), 3.94 (t, 8H, J = 6.5, Ph−OCH_{2-}), 3.94∼4.11 (m, 8H, crown ether(CH_2)), 6.84 (d, 8H, J = 8.6, O−Ph−H), 7.04 (s, 8H, cyclohexyl−Ph−H), 7.11 (d, 8H, J = 8.6, Ar−H (3,3′,7,7′)), 7.43 (d, 4H, J = 8.9, Ar−H (4,4′)), 7.64 (s, 4H, Ar−H (5,5′)), 7.88 (d, 4H, J = 9.0, Ar−H (8,8′)).

5.6. (*R*)-Crown(2)-(6,6′-PCH506-Binol) (*R*-6). ^{1}H NMR ($CDCl_3$, δ from TMS, ppm): 0.83∼1.84 (m, 56H, $-CH_3$, $-CH_{2-}$, cyclohexyl−H), 2.36 (t, 2H, J = 12.0, Ph−cyclohexyl−H), 2.67 (t, 4H, J = 7.6, Ar−CH_{2-}), 3.31∼3.79 (m, 4H, crown ether (CH_2), 3.81∼3.89 (m, 4H, crown ether ($-CH_{2-}$), 3.88 (t, 4H, J = 6.4, Ph−OCH_{2-}), 4.12∼4.44 (m, 4H, crown ether (CH_2)), 6.77 (d, 4H, J = 8.6, O−Ph−H), 6.98∼7.22 (m, 8H, cyclohexyl−Ph−H, Ar−H (3,3′,7,7′)), 7.31 (d, 2H, J = 9.1, Ar−H (4,4′)), 7.58 (s, 2H, Ar−H (5,5′)), 7.82 (d, 2H, J = 9.1, Ar−H (8,8′)).

5.7. (*R*)-Crown(2)-(6,6′-PCH5012-Binol) (*R*-7). ^{1}H NMR ($CDCl_3$, δ from TMS, ppm): 0.86−1.87 (m, 80H, $-CH_3$, $-CH_{2-}$, cyclohexyl−H), 2.39 (t, 2H, J = 12.1, Ph−cyclohexyl−H), 2.67 (t, 4H, J = 7.6, Ar−CH_{2-}), 3.54−3.73 (m, 8H, crown ether (CH_2)), 3.90 (t, J = 6.5, Ph−OCH_{2-}), 4.13−4.46 (m, 4H, crown ether (CH_2)), 6.80 (d, 4H, J = 8.6, O−Ph−H), 6.99−7.10 (m, 8H, cyclohexyl−Ph−H, Ar−H (3,3′,7,7′)), 7.32 (d, 2H, J = 9.1, Ar−H (4,4′)), 7.60 (s, 2H, Ar−H (5,5′)), 7.84 (d, 2H, J = 9.1, Ar−H (8,8′)).

Acknowledgment. This work was supported by a Grant-in-Aid for Science Research in a Priority Area “Super-Hierarchical Structures” (No. 446) from the Ministry of Education, Culture, Sports, Science and Technology, Japan. The authors are grateful for experimental supports of Messrs. Satoshi Matsushita and Takayuki Matsushita.

JA051548E